

Kinetic Isotope Effect Studies of the Reaction Catalyzed by Uracil DNA Glycosylase: Evidence for an Oxocarbenium Ion–Uracil Anion Intermediate[†]

R. Marshall Werner and James T. Stivers*

Center for Advanced Research in Biotechnology of the University of Maryland Biotechnology Institutes and
National Institute of Standards and Technology, 9600 Gudelsky Drive, Rockville, Maryland 20850

Received August 2, 2000; Revised Manuscript Received September 25, 2000

ABSTRACT: The DNA repair enzyme uracil DNA glycosylase catalyzes the first step in the uracil base excision repair pathway, the hydrolytic cleavage of the *N*-glycosidic bond of deoxyuridine in DNA. Here we report kinetic isotope effect (KIE) measurements that have allowed the determination of the transition-state structure for this important reaction. The small primary ¹³C KIE ($=1.010 \pm 0.009$) and the large secondary α -deuterium KIE ($=1.201 \pm 0.021$) indicate that (i) the glycosidic bond is essentially completely broken in the transition state and (ii) there is significant sp² character at the anomeric carbon. Large secondary β -deuterium KIEs were observed when $[2'R\text{-}^2\text{H}] = 1.102 \pm 0.011$ and $[2'S\text{-}^2\text{H}] = 1.106 \pm 0.010$. The nearly equal and large magnitudes of the two stereospecific β -deuterium KIEs indicate strong hyperconjugation between the elongated glycosidic bond and both of the C2'–H2' bonds. Geometric interpretation of these β -deuterium KIEs indicates that the furanose ring adopts a mild 3'-exo sugar pucker in the transition state, as would be expected for maximal stabilization of an oxocarbenium ion. Taken together, these results strongly indicate that the reaction proceeds through a dissociative transition state, with complete dissociation of the uracil anion followed by addition of water. To our knowledge, this is the first transition-state structure determined for enzymatic cleavage of the glycosidic linkage in a pyrimidine deoxyribonucleotide.

The enzymatic hydrolysis of the glycosidic bond in damaged DNA nucleotides is a critical first step in the repair of premutagenic lesions in DNA. A variety of highly specific enzymatic glycosidase activities have evolved to perform such repair reactions on alkylated, oxidized, or deaminated bases (1). Of these reactions, the most chemically difficult to carry out is the hydrolysis of the glycosidic bond in damaged pyrimidine nucleotides. One of the most frequent types of damage to a pyrimidine base in DNA is the spontaneous deamination of cytosine to generate uracil. Such events are unavoidable in the aqueous cellular environment, and are repaired by the highly conserved activity of the enzyme uracil DNA glycosylase (UDG,¹ Figure 1) (2).

Crystallography (3–5), NMR (6–8), and mechanistic studies (9, 10) have been used to extensively characterize UDG. This body of work has shown that catalysis first involves flipping the deoxyuridine nucleotide from the DNA helix into the enzyme active site. Once the nucleotide is inside the active site environment, the hydrogen bonding groups on the uracil base, as well as the 3' and 5' phosphodiester groups flanking the deoxyuridine nucleotide, form highly specific and catalytically important interactions with enzyme side chain groups (4, 5). The role of these

interactions in lowering the activation barrier likely involves discrete ground-state and transition-state contributions. Recent Raman studies have provided evidence for ground-state activation of the uracil leaving group through polarization of the carbonyl moieties of the uracil base (11). In addition, the crystal structure of UDG bound to DNA containing the C-glycoside substrate analogue, deoxypseudouridine, shows that the enzyme flattens the deoxyuridine sugar pucker in the ground state, thereby preorganizing the substrate into a conformation that would be expected to stabilize a transition state or intermediate that resembles an oxocarbenium ion (4). Two chemical groups have been strongly implicated in transition-state stabilization by kinetic, NMR, and mutagenesis studies (6, 8, 9). His187 has been shown by NMR to donate a short strong hydrogen bond to uracil O2, thereby lowering the N1 pK_a by 3.4 units as compared to that in solution, and facilitating the departure of the leaving group (7). A second group, Asp64, is well positioned to orient or accept a proton from the water molecule that attacks at C1' (6, 9). UDG is remarkable in that its 10¹²-fold catalytic power is obtained from a very limited set of binding interactions that allow it to work with equal facility on double-stranded and single-stranded dU DNA but not RNA (10).

Although the transition-state structure for enzymatic cleavage of the glycosidic bond in purine ribonucleosides has been determined for a number of enzymes (12), the structure for hydrolytic cleavage of the glycosidic bond in a pyrimidine deoxynucleotide in DNA is unknown. There are two possible transition-state extremes for the UDG-catalyzed reaction. The first is the formation of a discrete oxocarbenium intermediate

[†] This work was supported by NIH Grant RO1 GM56834 (J.T.S.) and the National Institute for Standards and Technology.

* To whom correspondence should be addressed. Phone: (301) 738-6264. Fax: (301) 738-6255. E-mail: stivers@carb.nist.gov.

¹ Abbreviations: UDG or *e*UDG, *Escherichia coli* uracil DNA glycosylase; pdU*dAddG, 5'-phosphorylated DNA trinucleotide with various radiolabels and isotopic labels in dU.

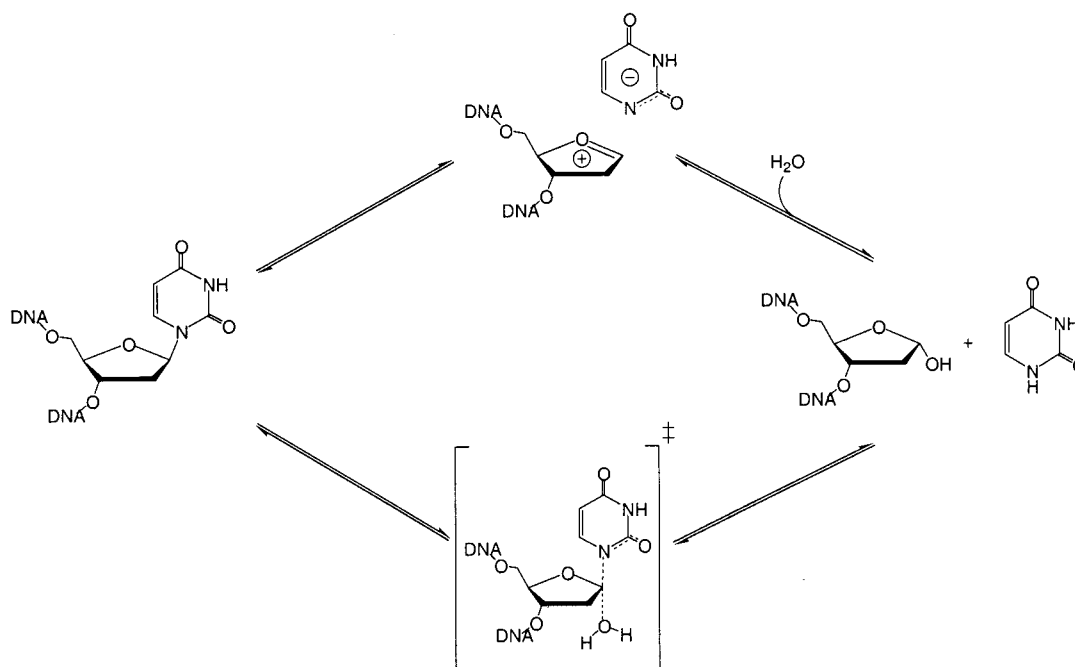


FIGURE 1: Possible reaction mechanisms for uracil DNA glycosylase (UDG). The top pathway illustrates a limiting stepwise mechanism involving the formation of a discrete oxocarbenium ion intermediate that is subsequently trapped by the water nucleophile. The bottom pathway illustrates an associative S_N2 mechanism involving concerted addition of the water nucleophile and expulsion of the uracil leaving group. The S_N2 mechanism may be further distinguished by the degree of dissociative character in the transition state.

with an sp^2 hybridized anomeric carbon (Figure 1, upper pathway). The second is the concerted association and dissociation of the nucleophile (water) and the leaving group (uracil) at the anomeric carbon (Figure 1, lower pathway). Although enzymatic hydrolysis of purine ribonucleosides has been generally shown to proceed through highly dissociative transition states, or even discrete oxocarbenium ion intermediates (13–15), it is not clear that pyrimidine deoxynucleotides would follow similar pathways due to the large differences in the chemical nature of the purine and pyrimidine leaving groups. These questions make a detailed study of the transition state of the UDG-catalyzed reaction of general mechanistic interest.

Kinetic isotope effect measurements (KIEs) are the only experimental approach that allows direct determination of transition-state structure for a given chemical reaction. The approach is to measure the differential reaction rates ($k_{\text{light}}/k_{\text{heavy}}$) for a substrate with light and heavy isotope substitutions at a specific atom or atoms that undergo a change in vibrational environment between the reactant state and the transition state of the reaction (12, 16). Thus, KIEs report directly on the relative “tightness” of bonding modes in the reactant and transition states. If a given bond becomes looser in the transition state than it is in the reactant state, leading to a lower vibrational frequency, then a “normal” KIE will result ($k_{\text{light}}/k_{\text{heavy}} > 1$). Conversely, inverse KIEs ($k_{\text{light}}/k_{\text{heavy}} < 1$) indicate that the bonding environment has become stiffer in the transition state. Here we report KIE studies on the reaction catalyzed by UDG in which we have probed the changes in vibrational environment for a number of isotopically sensitive sites within a deoxyuridine nucleotide in DNA. These data, in combination with recent crystallographic and NMR evidence, provide strong support for a reaction mechanism involving the formation of a discrete oxocarbenium ion–uracil anion intermediate. To our knowledge, this is the first example in which glycosidic bond

cleavage in a nucleoside has been shown to proceed through an ion pair intermediate.

EXPERIMENTAL PROCEDURES²

Materials. α -Ketoglutarate, β -NADH, β -NADP⁺, β -NADPH, uracil, [5-³H]uracil (specific activity of 12.0 Ci/mmol), ATP, dATP, glucose, 5'-deoxyadenosylcobalamin (coenzyme B₁₂), nucleoside diphosphate kinase (NDK) from bovine liver (EC 2.7.4.6), 6-phosphogluconic acid dehydrogenase (6-PGDH) from yeast (EC 1.1.1.44), phosphoribosylisomerase (PRI) from torula yeast (EC 5.3.1.6), and Q-Sepharose anion-exchange resin were from Sigma. Myokinase (MK) from rabbit muscle (EC 2.7.4.3), pyruvate kinase (PK) from rabbit muscle (EC 2.7.1.40), glutamate dehydrogenase (GDH) from beef liver (EC 1.4.1.3), lyophilized hexokinase (HK) from yeast (EC 2.7.1.1), and lyophilized glucose-6-phosphate dehydrogenase (G6PDH) from yeast (EC 1.1.1.49) were from Boehringer Mannheim/Roche. T4 polynucleotide kinase (PNK) (EC 2.7.1.78) was from New England Biolaboratories. [5-³H]dUTP (specific activity of 16.0 or 14.0 Ci/mmol) and dideoxyguanosine triphosphate (ddGTP) were from Amersham Life Sciences. [2-¹³C]-D-Glucose, [2-²H]-D-glucose, and D₂O were from Cambridge Isotope Laboratories. [2-¹⁴C]-Uracil (specific activity of 55 mCi/mmol) was from American Radiolabeled Chemicals, Inc. Ready Safe liquid scintillation fluid was from Beckman Instruments. Centriprep 3000 molecular weight cutoff (MWCO) centrifugal filters were from Amicon. The in-line scintillation analyzer was from Berthold. QE-20 anion-exchange resin was from

² Certain commercial equipment, instruments, and materials are identified in this paper to specify the experimental procedure. Such identification does not imply recommendation or endorsement by the National Institute of Standards and Technology, nor does it imply that the material or equipment identified is necessarily the best available for the purpose.

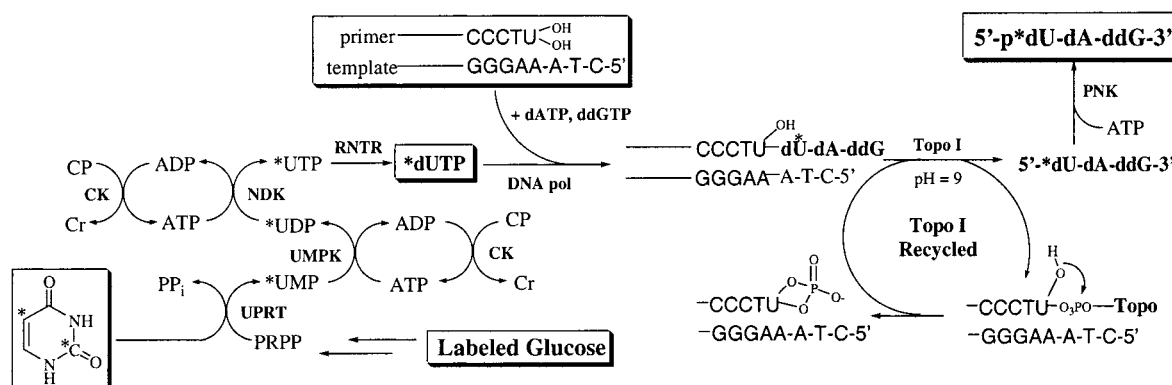


FIGURE 2: Enzymatic synthesis of isotopically labeled DNA. Through the action of 16 different enzymes, the synthesis of specifically labeled KIE substrates is accomplished in approximately 60% overall yield beginning from the precursors glucose and uracil. For the synthesis of substrates requiring deuterium in the 2'-H positions of the deoxyribose ring, D₂O was used as the solvent at appropriate steps in the synthesis (see the Supporting Information): UPRT, uracil phosphoribosyltransferase; UMPK, uracil monophosphate kinase; NDK, nucleoside diphosphate kinase; RNTR, ribonucleotide triphosphate reductase; DNA pol, DNA polymerase I Klenow fragment (exo⁻); Topo I, vaccinia type I topoisomerase; PNK, polynucleotide kinase; CK, creatine kinase; CP, creatine phosphate; CR, creatine.

Perceptive Biosystems. Disposable micro-spin plastic columns were from Bio-Rad. Phenomenex AQUA reverse-phase HPLC columns (analytical, 250 mm × 4.6 mm; preparative, 250 mm × 10 mm) were from Phenomenex (Torrance, CA). TN buffer consists of 60 mM NaCl and 20 mM Tris-HCl (pH 8.0).

Oligodeoxynucleotides were synthesized using an Applied Biosystems 390 synthesizer using standard phosphoramidite chemistry. All nucleoside phosphoramidites were purchased from Glen Research (Sterling, VA). After synthesis and deprotection, the oligodeoxynucleotides were purified by anion-exchange HPLC and desalted by reverse-phase HPLC (for oligonucleotides with fewer than eight nucleotides) or by gel filtration chromatography (for oligonucleotides with more than eight nucleotides). The concentrations were determined by UV absorption measurements at 260 nm, using the pairwise extinction coefficients for the constituent nucleotides (17).

Enzymes. The expression and purification of *e*UDG has been described previously (10, 18). The bacterial constructs for the overexpression of the enzymes uracil monophosphate kinase (UMPK), uracil phosphoribosyltransferase (UPRT), and phosphoribosylpyrophosphate synthase (PRPPS) were kindly provided by O. Barzu (Institut Pasteur, Paris, France) (19). Purification of UMPK and UPRT closely followed the procedures of Barzu (20) and Jensen (21), respectively. Purification of PRPPS followed the procedure of Switzer with several modifications (22). Crude cell lysate was applied to 6 g of Sepharose-bound blue dextran (Pharmacia Biotech) equilibrated with 50 mL of binding buffer (0.1 M triethanolamine, 0.1 M potassium phosphate, 0.75 mM EDTA, and 2 mM MgCl₂) at 4 °C. After being washed with 5 column volumes of 50 mM potassium phosphate (pH 7.7) to remove triethanolamine, the enzyme was eluted with 50 mM potassium phosphate (pH 7.7) containing 25 mM ATP and 25 mM MgCl₂. Fractions containing protein were quantitated using the Bradford reagent (23), pooled, and concentrated using an Amicon high-pressure protein concentration apparatus and a 10 000 MWCO filter. The concentrated protein was then dialyzed against 0.5 M potassium phosphate (pH 7.7) and stored at -80 °C in small single-use aliquots as there is significant loss of activity after repetitive freeze-thaw cycles. PRPPS was assayed using a spectrophotometric

assay involving the pyruvate kinase/lactate dehydrogenase coupling system by following the decrease in absorbance of NADH at 340 nm over time. *Escherichia coli* strain HB101/pSQUIRE used for the overexpression of *Lactobacillus leichmannii* ribonucleotide triphosphate reductase (RNTR) was provided by J. Stubbe. RNTR was purified and assayed as described by Stubbe (personal communication) (24, 25). Final protein stocks were stored at -80 °C in 0.1 M sodium citrate, 1 mM EDTA, 1 mM β-mercaptoethanol, 0.025% NaN₃, and 20% glycerol at pH 5.6 in 500 μL aliquots, and showed little loss of activity even after 1 year. The bacterial construct for overexpression of the Klenow fragment of DNA polymerase I (exo⁻) was provided by C. Joyce (Yale University, New Haven, CT) and was purified as described previously (26). Vaccinia type I topoisomerase was expressed and purified as previously described (27).

Enzymatic Preparation and NMR Characterization of Labeled dUTP and Incorporation into DNA. The detailed methods for the synthesis and characterization of the labeled dUTPs and the isotopically labeled DNA are described in the Supporting Information. Briefly, the enzymatic synthesis of isotopically labeled dUTP is accomplished through the sequential action of hexokinase, glucose-6-phosphate dehydrogenase, 6-phosphogluconate dehydrogenase, phosphoriboisomerase, 5-phosphoribosyl-1-pyrophosphate synthetase, uracil phosphoribosyltransferase, uridine monophosphate kinase, nucleoside diphosphate kinase, and ribonucleotide triphosphate reductase as outlined in Figure 2. In the approach used here, stable isotopes (1'-¹³C, 1'-²H, 2'-²H, and 2'-³H) were placed in the deoxyribose using the appropriately labeled glucose precursor, and the ³H and ¹⁴C radiolabels were placed in the 5 and 2 positions of the uracil base, respectively. The fractional stable isotope substitution of the labeled dUTPs was determined by NMR spectroscopy and was in the range 86–97% (see the Supporting Information).

The labeled trinucleotide for use in the KIE studies was enzymatically synthesized using the Klenow fragment of DNA polymerase I (exo⁻) starting from labeled dUTP*, dATP, and ddGTP as shown in Figure 2. The use of a 2'-hydroxyribonucleotide on the 3' end of the primer sequence allowed release of the 5'-hydroxytrinucleotide product through the site specific ribonuclease activity of the vaccinia

type I topoisomerase, which cleaves at the 5'-CCCTrU↓-3' sequence of the primer (28). Three orthogonal HPLC purification steps were required to achieve the high purity of labeled DNA required for KIE analysis (see the Supporting Information).

KIE Experiments. Reaction mixtures used for the determination of competitive isotope effects contained approximately 3 μM DNA in 200 μL of TN buffer with ~ 10000 cpm (300 pmol) of ^{14}C disintegrations per minute and ~ 20000 cpm (30 pmol) of ^3H disintegrations per minute. The reactions were initiated by the addition of 20 pmol of UDG (100 nM), and the mixtures were incubated at 37 $^\circ\text{C}$. Reactions were quenched after 1 min by the transfer of 97 μL of the reaction mixture to 353 μL of cold 10 mM NH_4HCO_3 (pH 4.0) which stopped hydrolysis at approximately 40% conversion. The remaining reaction mixture was allowed to react a total of 60 min to complete the hydrolysis of uracil, and 97 μL was transferred to 353 μL of cold 10 mM NH_4HCO_3 (pH 4.0). To separate labeled uracil from labeled DNA, the 450 μL solution was applied to either (i) an anion-exchange HPLC column (Poros QE-20, Perceptive Biosystems) equipped with an Berthold in-line scintillation counter or (ii) a disposable anion-exchange spin column [Bio-Rad micro-spin columns containing a 500 μL bed of Q-Sepharose (Sigma)]. For the HPLC assay, the following solvent gradient was used: flow rates of 1.5 mL/min for aqueous solvent and 3.0 mL/min for scintillation fluid, from 0 to 5 min isocratic buffer A (10 mM NH_4OAc), and from 5 to 9 min 0 to 100% buffer B (1 M NH_4OAc). For the spin column assay, after the quenched aqueous reaction mixture was allowed to flow through the spin column by gravity, three separate 1 mL washes of 10 mM Tris-HCl (pH 8.0) were collected directly by centrifugation into scintillation vials (Beckman TJ-6, 2 min at 2000 rpm). Both methods efficiently separate the DNA substrate from the product uracil and give identical KIE results. The HPLC method, although more tedious, was preferred because small amounts of substrate (0.1–0.2%) would sometimes coelute with the uracil product with the spin column method.

The resulting aqueous mixtures for each individual reaction containing both 5- ^3H - and 2- ^{14}C -labeled uracil at ~ 40 and 100% hydrolysis, respectively, were collected directly into scintillation vials and weighed. Care was taken to collect the entire radioactive peak. Scintillation fluid was added (~ 15 mL) such that the mixture was clear to improve counting efficiency. The vials were adjusted to identical weights with additional scintillation fluid to negate any differences in quenching effects between samples. A [5- ^3H]-uracil standard, a [2- ^{14}C]-uracil standard, and a blank vial were also counted each time the KIEs were measured to ensure no quenching effects were altering the observed KIEs. The samples were counted such that at least 300 000 total counts were measured in the ^3H and ^{14}C channels (10×20 min cycles). The blank was then subtracted from the experimental counts; the experimental values were averaged, and the observed KIE was calculated according to eq 1

$$\text{KIE}_{\text{obs}} = (^3\text{H}/^{14}\text{C})_{f_{\text{hyd}}} / (^3\text{H}/^{14}\text{C})_{100} \quad (1)$$

where $(^3\text{H}/^{14}\text{C})_{f_{\text{hyd}}}$ and $(^3\text{H}/^{14}\text{C})_{100}$ are the observed counting ratios at partial hydrolysis ($f_{\text{hyd}} = 0.3\text{--}0.7$) and complete conversion, respectively. Corrections for the fractional

isotopic substitution were made using eq 2, where f_{iso} is the percent isotopic substitution at a given site, and KIE_{obs} was corrected to zero fraction reaction using eq 3, where f_{hyd} is the fractional conversion (29, 30).

$$\text{KIE}_{\text{iso}} = (\text{KIE}_{\text{obs}} - 1 + f_{\text{iso}})/f_{\text{iso}} \quad (2)$$

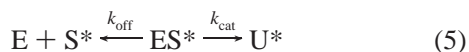
$$\text{KIE}_{\text{corr}} = \ln(1 - f_{\text{hyd}}\text{KIE}_{\text{iso}})/\ln(1 - f_{\text{hyd}}) \quad (3)$$

In eq 3, the fractional extent of the hydrolysis reactions (f) was determined by comparison of the ^{14}C counts per minute observed from samples quenched at 1 and 60 min [$f_{\text{hyd}} = \text{cpm}_{1\text{min}}/(\text{cpm}_{1\text{min}} + \text{cpm}_{60\text{min}})$]. Finally, corrections for the effect of the remote label ($\text{KIE}_{\text{ctrl}} = 1.00 \pm 0.011$) were made according to eq 4.

$$\text{KIE}_{\text{final}} = \text{KIE}_{\text{corr}}/\text{KIE}_{\text{ctrl}} \quad (4)$$

Steady-State Parameters for pdU^*dAddG . Reaction mixtures containing various concentrations of 5- ^3H -labeled substrate (4, 8, 12, 16, 32, and 64 μM) and a constant concentration of UDG (50 nM) were brought to a final volume of 20 μL using TN buffer. Reactions were quenched after 2 min ($\leq 10\%$ hydrolysis) by the addition of 20 μL of 1 N HCl and analyzed using the anion-exchange HPLC system equipped with an in-line scintillation counter (as described above). Integration of the resulting signals for radioactive uracil and substrate DNA was used to determine the fractional conversion to product at the time of quench [$\text{frac}_t = \text{cpm P}/(\text{cpm P} + \text{cpm S})$]. The steady-state kinetic parameters K_m and k_{cat} were obtained from plots of the initial velocities ($k_{\text{obsd}} = [\text{S}]_{\text{tot}}\text{frac}_t/t[\text{E}]$) versus substrate concentration using the Michaelis–Menten equation and the program GraFit 4 (31).

Pulse–Chase Substrate Partitioning Experiment. The extent to which enzyme-bound pdU^*dAddG is committed to the formation of product as opposed to being released to solution was measured by a pulse–chase substrate trapping experiment (12, 32). This experiment measures the partitioning ($k_{\text{cat}}/k_{\text{off}}$, eq 5) of ES^* between conversion to uracil (k_{cat} , eq 5) and dissociation to form free E and S^* (k_{off} , eq 5). The partitioning ratio $k_{\text{cat}}/k_{\text{off}}$ is measured by rapidly trapping the dissociated enzyme with a large excess of unlabeled single-stranded DNA 11mer (5'-GCGCAUAGTCG-3') and determining how much of the radioactivity initially present in the ES^* complex is found in the product uracil (U^*) and free S^* (eq 5).



Two reaction mixtures were prepared, each containing 40 μL of TN buffer and a substrate concentration of 40 μM (labeled pdU^*dAddG was diluted with unlabeled substrate DNA to obtain a final specific activity of 160 mCi/mmol). Each separate reaction was initiated by the addition of UDG to give a final enzyme concentration of 50 μM . The first reaction was quenched after 5 s with 40 μL of 1 N HCl. For the second reaction, instead of the acid quench, 40 μL of a 4.14 mM solution of the 11mer trap DNA was added 5 s after the addition of UDG. Aliquots (10 μL) were then removed periodically over the next 55 s and the reactions quenched with 10 μL of 1 N HCl. The quenched samples from both reactions were analyzed for fraction hydrolysis

$[U^*/(U^* + S^*)]$ using anion-exchange HPLC with in-line scintillation counting as described above.

Calculations. All structure optimizations and electrostatic potential calculations were performed using the program PC Spartan Pro 1.0.3 (Wavefunction Inc., Irvine, CA) using the Gaussian 6-31+G* basis set that incorporates diffuse functions.

RESULTS

Enzymatic Synthesis of Isotopically Labeled DNA

The KIE measurements required the synthesis of dU-containing single-stranded DNA with stable isotope substitutions in isotopically sensitive positions of the deoxyribose moiety of dU, and radioactive reporter groups in isotopically insensitive positions of the uracil ring (see below). An enzymatic approach for the synthesis of dUTP was utilized based on the procedure of Barzu and co-workers (19). Thus, in a single-pot reaction starting from the appropriate stable isotope-labeled glucose, and using commercially available 5-³H- or 2-¹⁴C-labeled uracil, specifically labeled dUTP was obtained in approximately 65% isolated yield (Figure 2). The following labeled molecules were synthesized using this method: [5-³H]dUTP, [2-¹⁴C]dUTP, [2-¹⁴C,1'-²H]dUTP, [2-¹⁴C,1'-¹³C]dUTP, [2-¹⁴C,2'-²H]dUTP, [2-¹⁴C,2'-³H]dUTP, and [5-³H,1'-²H]dUTP. Labeled dUTP was analyzed for purity by HPLC (>95%) and for percent isotopic substitution by NMR (90–97%; see the Supporting Information). In this synthesis, the ³H and ¹⁴C reporter labels are placed in the 5 and 6 positions of the uracil base, respectively, rather than the sugar because (i) in the KIE experiments it is easy to completely separate the uracil product from the DNA substrate using HPLC methods and (ii) the possibility of β and δ elimination reactions with the abasic DNA product makes the placement of tritium labels in the deoxyribose undesirable. Accordingly, the stable isotope labels are placed in the isotopically sensitive positions of the sugar (see Table 1). This labeling approach differs from that previously used for a number of ribonucleoside hydrolase reactions (12).

DNA polymerase was used to incorporate dUTP* into a DNA trinucleotide for the KIE studies (33). In this procedure, a DNA primer–template complex was designed with the vaccinia type I DNA topoisomerase consensus sequence 5'-CCCTrU↓-3' at the 3' end of the primer strand (Figure 2). The primer was then extended by three nucleotides using Klenow polymerase I (exo⁻), labeled dUTP*, dATP, and the terminator dideoxynucleotide ddGTP to ensure that extension beyond the trinucleotide was prevented (34). After separation of the labeled dsDNA from unincorporated dUTP* by size exclusion filtration, vaccinia topoisomerase I was added to catalytically release the labeled trimer utilizing its site specific ribonuclease activity (28) (Figure 2). Because this reaction was performed at pH 9.0, the covalent phosphotyrosine intermediate is cleaved through the attack of the 2'-hydroxyl, resulting in the formation of a 2'-3' cyclic phosphate at the 3'-terminus of the primer strand and releasing topoisomerase for further reaction. Quantitative phosphorylation of the 5'-terminus by polynucleotide kinase in the presence of ATP afforded the labeled trimer substrate, pdU*dAddG, in high yield ($\geq 80\%$ from dUTP). The use of topoisomerase cleavage dramatically improved yields of

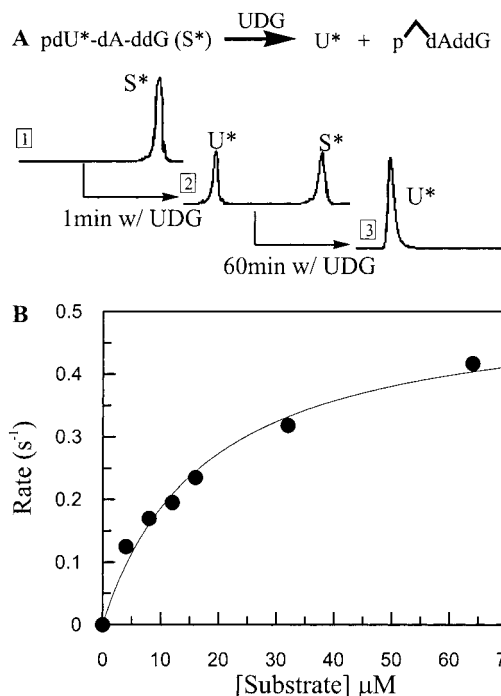


FIGURE 3: (A) HPLC assay for the separation of the labeled DNA substrate from the uracil product. An anion-exchange HPLC column with an in-line scintillation counter was used to separate and quantify labeled DNA and labeled uracil. After the reaction of labeled DNA (1) with UDG for 1 min, the hydrolysis reaction is approximately 40% complete (2). Upon reaction for 60 min, the hydrolysis to uracil is complete (3). (B) Kinetic parameters of labeled DNA. Kinetic parameters were obtained from the initial rates of uracil formation (50 nM UDG, [³H-labeled DNA] = 4, 8, 12, 16, 32, and 64 μM). $K_m = 18 \mu\text{M}$, and $k_{\text{cat}} = 0.51 \text{ s}^{-1}$.

labeled DNA when compared to the yields realized with the standard alkaline hydrolysis method (33). After HPLC purification, all substrates were reacted with UDG and analyzed by anion-exchange HPLC and in-line scintillation counting to show that the radiolabel was only in the uracil portion of the substrate (Figure 3A).

Determination of Steady-State Kinetic Parameters

The rational use of the competitive isotope effect technique requires that the chemical step of the reaction be rate-limiting. If any step in the enzymatic reaction is slower than the chemical step (i.e., product release or substrate binding), the KIE may be masked. Since UDG is an extremely efficient glycosylase, exhibiting diffusion-controlled binding and rate-limiting product release for good substrates (10), it was imperative to find a substrate that overcame these problems. After careful screening of many substrate constructs (data not shown), a trinucleotide substrate of the sequence pdU*dAddG was found to fit the necessary criteria. From initial rate analysis as a function of substrate concentration (Figure 3B), steady-state kinetic parameters for pdU*dAddG were determined: $K_m = 18 \pm 3 \mu\text{M}$, $k_{\text{cat}} = 0.51 \pm 0.03 \text{ s}^{-1}$, and $k_{\text{cat}}/K_m = 0.028 \pm 0.005 \mu\text{M}^{-1} \text{ s}^{-1}$. For comparison, the optimal 4mer dU containing the ssDNA sequence AUAA has a K_m of 1 μM , a k_{cat} of 15 s^{-1} , and a single-turnover k_{max} of 110 s^{-1} (Y. L. Jiang and J. T. Stivers, unpublished observations). Thus, uracil is released from the trinucleotide at a rate that is about 200-fold slower than that of the optimal substrate AUAA (110 $\text{s}^{-1}/0.51 \text{ s}^{-1}$). Although this is a

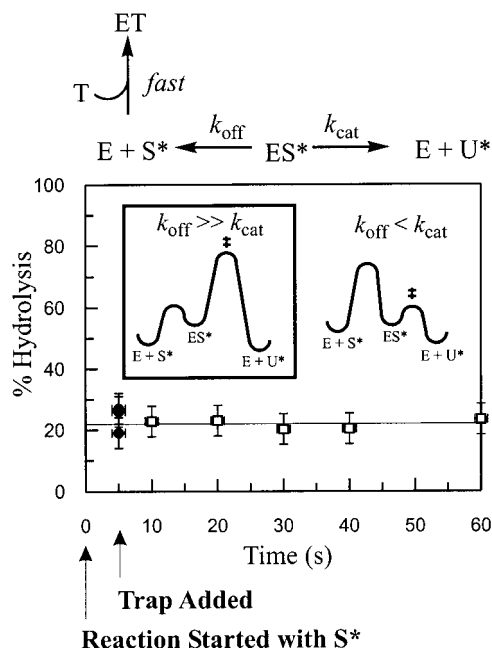


FIGURE 4: Substrate trapping experiment to determine the forward commitment to catalysis. UDG was mixed with p -[5- ^3H]dUdAddG DNA in the pulse phase for 5 s in two separate reactions. The individual reactions were either (i) terminated with acid at 5 s and analyzed for uracil formation (●) or (ii) diluted with a chase solution containing a large excess of unlabeled 11mer DNA. After addition of the chase solution, aliquots were removed at the indicated times and analyzed for uracil formation (□). Labeled product is no longer formed after addition of the DNA trap at 5 s, indicating that S^* dissociation from ES^* is much more rapid than conversion to U^* . On the basis of the upper limit errors in the measurements, we estimate that the commitment factor is less than 5%, which indicates that the observed isotope effects are intrinsic.

significant difference in rates, it is small compared to the total catalytic power of UDG (10^{12}), indicating that a majority of the binding interactions required for catalysis are preserved in this trinucleotide substrate. In addition, we have previously shown that a similar trinucleotide substrate had the same pH dependence for k_{cat} as an optimal 5mer substrate, which indicates the same chemical groups are involved in catalysis of bond cleavage for both substrates (9).

Forward Commitment to Catalysis

The forward commitment to catalysis is defined as the fraction of the substrate in the Michaelis complex that partitions forward to product as opposed to dissociation to form free substrate and enzyme ($k_{\text{cat}}/k_{\text{off}}$; Figure 4). If k_{cat} is significantly greater than the off-rate (i.e., a large forward commitment exists), the KIE on $k_{\text{cat}}/K_{\text{m}}$ will be partially or completely obscured and will not directly reflect bonding changes in the transition state (35). To obtain information on the $k_{\text{cat}}/k_{\text{off}}$ ratio, we employed the substrate partitioning method developed by Rose (32). In this experiment, a Michaelis complex with a radiolabeled substrate (ES^*) is first formed in a pulse phase, and this complex is rapidly mixed with a large excess of the unlabeled dU–DNA species in a chase phase to trap the free enzyme after release of S^* . Thus, if dissociation of S^* is much more rapid than the rate constant for proceeding to product, no labeled product (U^*) will be formed after addition of the DNA chase solution. As shown in Figure 4, addition of the chase solution 5 s after formation of the ES^* complex resulted in no more U^*

formation than addition of an acid quench at 5 s. Thus, the chemical step is much slower than release of S^* , indicating that the KIEs will not be obscured by an unfavorable forward commitment factor. An upper limit to the $k_{\text{cat}}/k_{\text{off}}$ ratio of $\leq 1/20$ was determined on the basis of the 5% errors in the measurements shown in Figure 4. Thus, from these data, k_{off} is greater than $(0.51)(20)$ or $>10 \text{ s}^{-1}$. This lower limit is consistent with the previously determined off-rate of 42 s^{-1} for a 19mer dU-containing DNA substrate analogue (10).

We were not able to detect any incorporation of U^* in DNA by incubation of UDG with the abasic DNA product in the presence of high concentrations of U^* (data not shown). This result indicates that the glycosidic bond cleavage step is essentially irreversible and that the enzyme-bound products do not revert back to substrate.

KIE Measurements

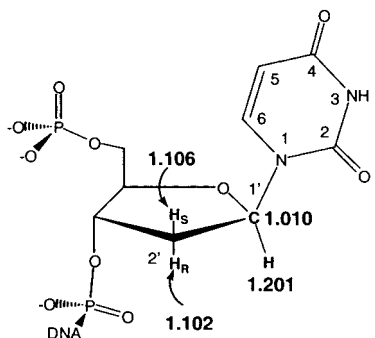
The KIE is defined as the ratio of the reaction rate constants for a heavy and light isotope-substituted substrate ($k_{\text{light}}/k_{\text{heavy}}$). Although in some cases the reaction rates k_{light} and k_{heavy} may be determined in separate reactions, it is preferable, when measuring small KIEs, to use the competitive dual-label method (29). In the implementation of the approach used here, the substrates containing [2- ^{14}C]uracil report on k_{heavy} (where the heavy isotope is 1'- or 2'- ^2H or 1'- ^{13}C), while those containing 5- ^3H report on the rate of light isotope (1'- or 2'- ^1H or 1'- ^{12}C). Thus, the 1'- ^2H secondary isotope effect can be measured by mixing the 2- ^{14}C - and 1'- ^2H -labeled substrate with the 5- ^3H - and 1'- ^1H -labeled substrate and comparing the $^{14}\text{C}/^3\text{H}$ ratio of the uracil product at partial and complete conversions to product (36). Normal isotopic discrimination against the heavy label results in a decreased $^{14}\text{C}/^3\text{H}$ ratio at partial conversion, which may be compared with the ratio at complete conversion to obtain the KIE (there is no isotopic discrimination in the product at 100% conversion). In Table 1 are reported the α -secondary 1'-deuterium, primary 1'- ^{13}C , and stereospecific β -secondary deuterium KIEs for the UDG reaction.

We were unable to determine the isotope effects for the nonenzymatic cleavage of the glycosidic bond of deoxyuridine, due to extensive loss of the 5-tritium label at the high temperatures, long incubation times, and acidic conditions used to assess the uncatalyzed reaction. In addition, the enzymatic 1- ^{15}N KIE was not measured because the synthesis of ^{15}N -labeled uracil unavoidably incorporates ^{15}N into both the 1 and 3 positions (19), which would complicate the interpretation of the isotope effect unless assumptions were made.

KIE Control Experiments

In addition to confirmation that the KIEs were not compromised by unfavorable forward or reverse commitment factors (see above), the following key controls were performed.

No Isotope Partitioning of Labeled Uracil during Chromatography. To demonstrate that the chromatographic separation of uracil from labeled DNA does not introduce errors due to differential partitioning of [5- ^3H]- and [2- ^{14}C]-uracil during chromatography, the following experiment was performed. A mixture of 5- ^3H - and 2- ^{14}C -labeled pdU*dAddG was incubated with UDG for 60 min to completely convert

Table 1: Kinetic Isotope Effects for UDG-Catalyzed Cleavage of Uracil from DNA^a


isotope positions	origin of KIE	exptl KIEs ^b
[2- ¹⁴ C]-1'- ² H, [5- ³ H]	α -secondary ² H	1.201 \pm 0.021 (15, 4, 3)
[2- ¹⁴ C]-1'- ¹³ C, [5- ³ H]	primary ¹³ C	1.010 \pm 0.009 (14, 4, 3)
[2- ¹⁴ C]-2'- ² H, [5- ³ H]	β -secondary ² H	1.102 \pm 0.011 (9, 4, 2)
[2- ¹⁴ C]-2'- ² H, [5- ³ H]	β -secondary ² H	1.106 \pm 0.012 (9, 4, 2)
[2- ¹⁴ C], [5- ³ H]	control	1.000 \pm 0.011 (19, 4, 3)

^a Substrate isotope positions are shown in the structure, and the associated KIEs and errors are reported herein. ^b The numbers in parentheses represent (i) the total number of independent measurements of the KIE, (ii) the number separate syntheses beginning from labeled dUTP*, and (iii) the number of separate syntheses beginning from labeled glucose and uracil.

the labeled substrate to product. Half of the reaction mixture was then purified by HPLC and placed into a scintillation vial, while the other half was placed directly into a scintillation vial. The ³H/¹⁴C ratio for both samples was measured using scintillation counting. The sample that was subjected to the chromatographic procedure gave a ³H/¹⁴C ratio of 7.4530, as compared to a value of 7.4529 for the untreated sample. Therefore, no isotopic partitioning between [5-³H]- and [2-¹⁴C]uracil occurs during chromatography. An identical result was obtained with the spin column procedure.

Confirmation of the Position of Stable Isotope Labels. The position and fractional substitution for each labeled dUTP were confirmed by ¹H and ¹³C NMR spectroscopy (see the Supporting Information). It is assumed that the position and fractional substitution of the 1'- and 2'-deuterium labels are unaltered upon incorporation into DNA, and during the subsequent cleavage, phosphorylation, and purification steps.

No Tritium Exchange during KIE Measurements. To exclude the possibility that the 5-³H label exchanged with solvent protons during the course of the KIE measurements, the pdU*dAddG substrate was incubated for 60 min in the absence of enzyme and then subjected to HPLC. No tritium counts were detected except in the position where the substrate elutes. In addition, we have found less than 0.5% tritium loss from our labeled substrates after storage for 3 months at -80 °C, indicating that the 5 position is fairly inert to exchange. Nevertheless, all the isotope effect measurements were made within 2–7 days of the initial HPLC purification of the DNA substrates.

The Entire Substrate Radioactivity Is in the Uracil Base. Each U*-containing trinucleotide substrate was incubated with UDG to demonstrate that 100% of the radioactivity was converted to uracil. In all cases, the reactions proceed to $\geq 99.5\%$ completion (see, for example, Figure 3A).

Adherence to the Bigeleisen Equation. Since the observed KIE changes over the course of the reaction due to isotopic

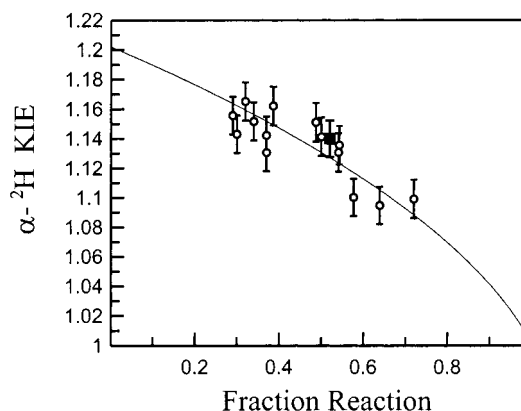


FIGURE 5: Demonstration that the observed KIEs adhere to eq 3 (30). For a normal KIE ($k_{\text{light}}/k_{\text{heavy}} > 1$), the heavier atom reacts more slowly than the light isotope; thus, as the reaction proceeds, the light isotope is depleted and leads to a decreasing apparent isotope effect as the reaction proceeds. Thus, the individual KIEs obtained at different fractional extents of reaction must be corrected to zero fractional conversion using eq 3 to obtain the intrinsic KIEs. The datum indicated with the black square was obtained with the ¹⁴C and ³H reporter labels switched (see the text).

discrimination, it is essential to correct the observed effects to zero fractional conversion using eq 3 derived by Bigeleisen (30). Figure 5 shows that the numerous measurements of the α -secondary ²H KIE at different fractional conversions to product are well fitted to the Bigeleisen equation, validating its use in correcting the KIEs to zero fractional conversion.

Identical KIEs Are Observed When the Radioactive Reporter Labels Are Switched. In the KIE measurements described above, ³H at the 5 position of uracil reports on the rate of the light isotope in the deoxyribose ring, while ¹⁴C at the C2 position of uracil reports on the rate of the heavy isotope. As shown in Table 1, these remote reporter labels in themselves produce no detectable KIE. However, to further confirm that the reporter labels did not influence the observed KIEs, the radioactive labels were switched in an experiment to determine the α -secondary ²H isotope effect. This was easily accomplished by altering the initial synthesis of dUTP by switching the radiolabeled bases (Figure 2). The observed α -secondary ²H KIE from this experiment was 1.190 after the appropriate corrections were applied (Figure 5, ■), which falls well within the error limits for the same measurements reported in Table 1 using the alternative reporter labels. The ability to switch labels demonstrates the synthetic utility of placing the radiolabel in the base rather than in the sugar, and provides confirmation of the reliability of the KIE measurements reported in Table 1.

DISCUSSION

Structural Characteristics of the Transition State. KIEs reflect bonding changes between a reactant state and the transition state, and therefore provide direct information about the extent of bond breakage and the geometric features of the transition state. There are two general approaches for the interpretation of the KIEs in terms of a transition-state structure. The first is the comparison of the KIEs with those of similar reactions in which the transition state is already known. The second is to use ab initio methods or ball-and-

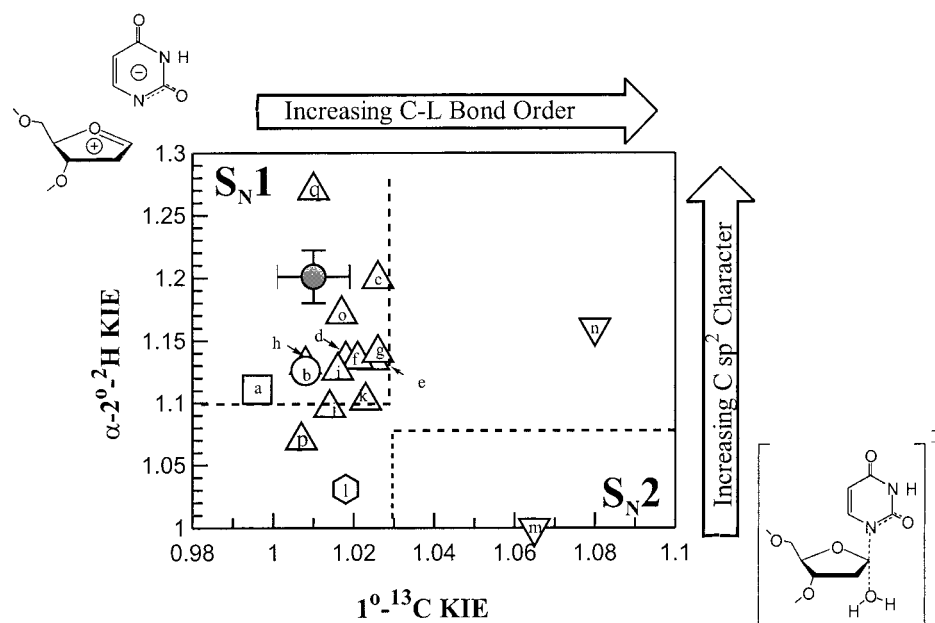


FIGURE 6: Mapping the transition state of the UDG reaction. A plot of primary ^{13}C isotope effects vs the α -secondary deuterium isotope effects for a number of glycosidic bond cleavage and related reactions. The observed value for UDG is plotted as a dark circle, while the other KIEs have been grouped into the following mechanistic categories: ricin/RNA (oxocarbenium ion intermediate) (\square), ricin/DNA (oxocarbenium ion intermediate) (\circ), assorted ribohydrolases ($\sim 95\%$ dissociative) (\triangle), ribohydrolase reactions with less $\text{S}_{\text{N}}1$ character (\circ), and reactions proceeding with an $\text{S}_{\text{N}}2$ mechanism (∇). The dashed lines represent the limits of transition-state space for dissociative ($\text{S}_{\text{N}}1$, upper left) and associative reactions ($\text{S}_{\text{N}}2$, lower right) (12, 46). Decreasing values of the primary ^{13}C KIEs represent a decrease in the level of bonding to the leaving group in the transition state, while increasing values of the $\alpha\text{-}^2\text{H}$ KIEs represent increasing amounts of sp^2 character at the anomeric carbon (i.e., increasing $\text{S}_{\text{N}}1$ character). Thus, stepwise $\text{S}_{\text{N}}1$ reactions fall in the upper left corner and associative $\text{S}_{\text{N}}2$ reactions in the lower left corner of the plot. In this compilation, reported ^{14}C and ^3H isotope effects have been corrected to ^{13}C and ^2H values using the equations ^{14}C KIE = ^{13}C KIE $^{1.90}$ and ^3H KIE = ^2H KIE $^{1.44}$, respectively (47). Letters inside the symbol correspond to the associated references: (a) ricin-catalyzed hydrolysis of RNA (13), (b) ricin-catalyzed hydrolysis of DNA (14), (c) hypoxanthine-guanine phosphoribosyl transferase (38), (d) NAD hydrolysis by diphtheria toxin (48), (e) ADP ribosylation of G_{act} subunits by pertussis toxin (49), (f) orotate phosphoribosyltransferase (50), (g) ADP ribosylation of G-peptide $\alpha_{13}\text{C}20$ by pertussis toxin (51), (h) NAD solvolysis (15), (i) NAD hydrolysis by cholera toxin (52), (j) inosine hydrolase (53), (k) nucleoside hydrolase from *Crithidia fasciculata* (54), (l) AMP nucleosidase (55), (m) glucopyranosyl fluoride hydrolysis (57), (n) S-adenosylmethionine synthase (56), (o) glucopyranosyl fluoride hydrolysis by glucoamylase (58), and (p) glucopyranosyl fluoride hydrolysis by sugar beet glucosidase (58).

spring vibrational models to calculate the KIEs for a transition state of known structure and then compare these calculated KIEs with the experimental KIEs (16). Since the interactions in the enzyme active site are likely to have a significant influence on the vibrational modes in the transition state or intermediate of a reaction, *ab initio* studies are most informative if performed in the context of the active site environment, which is beyond the scope of the current work. Therefore, we interpret the KIEs on the basis of comparison with those of other enzymatic glycosidase reactions, and limiting KIE values obtained from *ab initio* calculations in vacuo (13, 14).

The experimental KIEs unambiguously indicate that UDG stabilizes a dissociative transition state with substantial oxocarbenium ion character, and suggest that a short-lived oxocarbenium ion intermediate is formed on the enzyme (Table 1). The large and normal α -deuterium KIE of 1.201 indicates that the anomeric carbon has a large amount of sp^2 character in the transition state, resulting from a loosening of the out-of-plane bending mode for the anomeric proton in the planar transition state as compared to the tetrahedral reactant state. This α -deuterium KIE is similar to the maximum value of 1.197 for the equilibrium formation of an oxocarbenium ion calculated using *ab initio* methods (14).³ The small primary ^{13}C KIE of 1.010 is smaller than the lowest $1^\circ\text{-}^{13}\text{C}$ KIE calculated for highly dissociative $\text{S}_{\text{N}}2$ reactions (1.013–1.015) (14), strongly suggesting that uracil

departure and nucleophilic attack occur in distinct steps. The large stereospecific $2'\text{-}\beta$ -deuterium KIEs of 1.102 and 1.106 are also close to the maximal values calculated for the equilibrium formation of an oxocarbenium ion (1.140–1.159) (14). Such large β -deuterium KIEs indicate a highly dissociative transition state, because these effects arise from hyperconjugation from the $2'$ substituents to the electron deficient p orbital on the anomeric carbon in the nascent oxocarbenium ion. As will be discussed below, these β deuterium KIEs also provide information about the geometry of the deoxyribose ring in the transition state or oxocarbenium ion intermediate.

Mapping the UDG Transition State with Related Reactions. The primary carbon and α -deuterium KIEs have been measured for a number of ribohydrolases, one deoxyribohydrolase, phosphoribosyl transferases, and several other related reactions (Figure 6, where the details of the individual reactions are found in the legend). Since these two KIEs reflect strongly on the structure of the transition state, with small primary and large secondary effects corresponding to dissociative and stepwise mechanisms, respectively, a useful way to visualize the diversity of transition-state structures

³ All the KIEs that we report are for ^{13}C and ^2H . If calculations or experimental measurements from other studies used ^{14}C or ^3H , these values were corrected using the Swain–Schaad relationship (^{14}C KIE = ^{13}C KIE $^{1.9}$ and ^3H KIE = ^2H KIE $^{1.44}$) (47).

orbital—C1'—C2'—H2'_s dihedral angle to the calculated value of 30°. The resulting conformation is essentially indistinguishable from the flattened sugar conformation seen in the reactant-state crystal structure (4), suggesting that substrate preorganization plays a significant role in catalysis.

Is the Active Site Environment Consistent with a High-Energy Oxocarbenium Ion Intermediate? Since it is well-established that oxocarbenium ions derived from the hydrolysis of 2-hydroxy- and 2-deoxyribofuranosides have at most a borderline existence in solution (43–45), it is of interest to ask what features of the UDG active site lead to stabilization of such an intermediate. These features likely include the following:

(1) The use of binding energy to enforce a flattened sugar pucker in the ground state that maximizes the stabilizing hyperconjugative effects in the transition state and intermediate. This binding energy is likely derived from the interactions of the enzyme with the 5'- and 3'-phosphodiester groups, which drive the sugar pucker away from the 2'-endo conformation toward the flattened conformation seen in the Michaelis complex and the intermediate (Figure 7).

(2) Enzymatic stabilization of the uracil anion leaving group by formation of a short strong hydrogen bond to uracil O2 (6, 7). Heteronuclear NMR and Raman studies have shown that UDG lowers the N1 p*K*_a of the uracil leaving group by 3.4 units as compared to that in aqueous solution, resulting in the surprising finding that the uracil anion exists as a stable species in the active site at neutral pH. Such a stable anion in proximity to the cationic sugar would be expected to provide electrostatic stabilization of the intermediate. In addition, the decrease in the p*K*_a of the N1 position, and delocalization of the electron density to uracil O2, would also serve to diminish the reactivity of N1 as a nucleophile, thereby increasing the lifetime of the intermediate.

(3) Electrostatic stabilization of the cationic sugar by Asp64. The completely conserved active site residue, Asp64, is located on the α face of the sugar ring, with its γ oxygen located 3.36 Å from C1' of the deoxyuridine (4, 5). This group has been suggested either to act as a general base (p*K*_a = 6.5) for extraction of a proton from the water nucleophile (9) or simply to orient the nucleophile for attack on the oxocarbenium ion intermediate (6). The results presented here, which suggest the presence of an unstable intermediate, would seem to favor the latter role, because the attack of water on such a highly reactive intermediates does not require assistance from general base catalysis. The oxocarbenium ion intermediate is thus sandwiched between the negatively charged uracil anion and Asp64. Currently, we have no direct information for the fate of the proton that is derived from the attacking water. However, direct NMR measurements clearly establish that it does not reside on uracil N1 (7), which is contrary to previous assumptions.

The charge distributions in the free deoxyuridine reactant and in the oxocarbenium ion—uracil anion intermediate are shown in Figure 8 as electrostatic potentials projected onto the van der Waals surfaces of the molecules. In addition, the active site Asp64 is also included in the depiction shown in panel B. In this depiction of the reaction, the profound changes in charge distribution on the sugar and uracil base between the reactant state and intermediate are dramatically visualized. For UDG, the intermediate has a charge distribu-

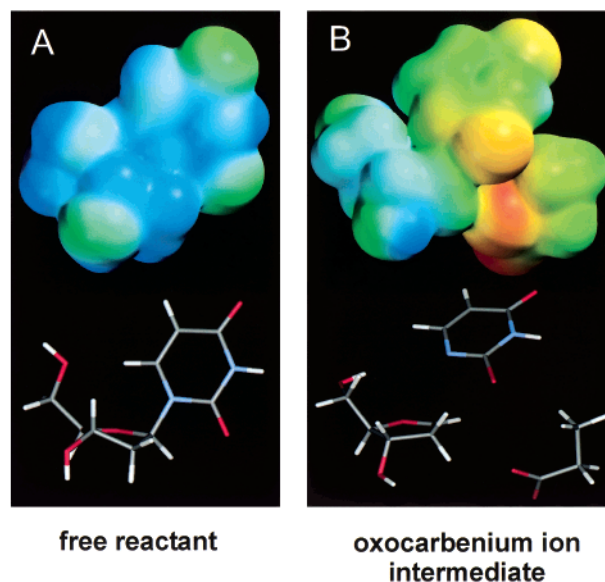


FIGURE 8: Electrostatic stabilization of the oxocarbenium ion intermediate in the active site of UDG. The electrostatic potentials for (A) the deoxyuridine reactant and (B) the oxocarbenium ion—uracil anion intermediate are projected onto the van der Waals surfaces for each molecule. For reference, the corresponding stick figures are shown below the structures. In addition, the active site Asp64 is also included in the depiction shown in panel B. The structure for 2'-endo deoxyuridine was obtained from the NMR structure of this residue in DNA (59), and the heavy atom coordinates for the uracil, abasic sugar, and Asp64 were obtained from the crystal structure of the ternary product complex of UDG (5). The oxocarbenium ion was energy optimized by fixing the O3' and O5' atoms and constraining the p orbital—C1'—C2'—H2'_s dihedral angle as determined from the KIEs. The uracil was optimized in the N1—O2 imidate form as determined from NMR measurements (7). Several factors likely contribute to the increased stability of the intermediate as compared to the stability in solution: (i) the enforcement of stabilizing hyperconjugative effects and (ii) electrostatic stabilization by the anionic uracil leaving group and Asp64 (6, 7).

tion distinctly different from that proposed for ricin-catalyzed cleavage of the *N*-glycosidic bond in adeosine (13). In the latter reaction, the adenine ring is proposed to be protonated at two sites, thereby enhancing leaving group departure and negating negative charge accumulation at N9. In contrast, the uracil base accumulates a full negative charge in the intermediate that is primarily localized on uracil O2 as determined by NMR (6, 7). As shown in Figure 8B, the electrostatic environment provided by the uracil anion and Asp64 effectively cradles the positive charge that accumulates on the sugar in the intermediate. These apparent mechanistic differences between enzyme-catalyzed hydrolysis of purine and pyrimidine bases further highlight how the intrinsic chemical properties of these bases influence the evolution of the enzyme mechanism (6, 7).

CONCLUSIONS

The UDG-catalyzed cleavage of the *N*-glycosidic bond in deoxyuridine occurs through a stepwise mechanism. The resulting oxocarbenium ion intermediate is stabilized through electrostatic interactions with the anionic uracil leaving group, Asp64, and by binding interactions that enforce a flattened sugar conformation that promotes stabilizing hyperconjugative effects in the intermediate. These results represent the first measurements of the transition-state

features for glycosidic bond hydrolysis in a pyrimidine deoxynucleoside and suggest that other DNA repair glycosylases should be amenable to this type of study.

ACKNOWLEDGMENT

We thank Drs. Octavian Barzu, Joanne Stubbe, and Cathy Joyce for supplying enzyme expression constructs, Dr. Alexander C. Drohat for help with the NMR experiments, and Drs. Vern Schramm and Paul Berti for helpful discussions and for providing results prior to publication.

SUPPORTING INFORMATION AVAILABLE

Detailed procedures for the enzymatic synthesis and NMR characterization of isotopically labeled dUTP and the trinucleotide DNA substrate. This material is available free of charge via the Internet at <http://pubs.acs.org>.

REFERENCES

- Mol, C. D., Parikh, S. S., Putnam, C. D., Lo, T. P., and Tainer, J. A. (1999) *Annu. Rev. Biophys. Biomol. Struct.* 28, 101–128.
- Mosbaugh, D. W., and Bennett, S. E. (1994) *Prog. Nucleic Acid Res. Mol. Biol.* 48, 315–370.
- Xiao, G., Tordova, M., Jagadeesh, J., Drohat, A. C., Stivers, J. T., and Gilliland, G. L. (1999) *Proteins* 35, 13–24.
- Parikh, S. S., Walcher, G., Jones, G. D., Slupphaug, G., Krokan, H. E., Blackburn, G. M., and Tainer, J. A. (2000) *Proc. Natl. Acad. Sci. U.S.A.* 97, 5083–5088.
- Parikh, S. S., Mol, C. D., Slupphaug, G., Bharati, S., Krokan, H. E., and Tainer, J. A. (1998) *EMBO J.* 17, 5214–5226.
- Drohat, A. C., and Stivers, J. T. (2000) *Biochemistry* 39, 11865–11875.
- Drohat, A. C., and Stivers, J. T. (2000) *J. Am. Chem. Soc.* 122, 1840–1841.
- Drohat, A. C., Xiao, G., Tordova, M., Jagadeesh, J., Pankiewicz, K. W., Watanabe, K. A., Gilliland, G. L., and Stivers, J. T. (1999) *Biochemistry* 38, 11876–11886.
- Drohat, A. C., Jagadeesh, J., Ferguson, E., and Stivers, J. T. (1999) *Biochemistry* 38, 11866–11875.
- Stivers, J. T., Pankiewicz, K. W., and Watanabe, K. A. (1999) *Biochemistry* 38, 952–963.
- Dong, J., Drohat, A. C., Stivers, J. T., Pankiewicz, K. W., and Carey, P. R. (2000) *Biochemistry* 39 (in press).
- Schramm, V. L. (1999) *Methods Enzymol.* 308, 301–354.
- Chen, X.-Y., Berti, P. J., and Schramm, V. L. (2000) *J. Am. Chem. Soc.* 122, 1609–1617.
- Chen, X.-Y., Berti, P. J., and Schramm, V. L. (2000) *J. Am. Chem. Soc.* 122, 6527–6534.
- Berti, P. J., and Schramm, V. L. (1997) *J. Am. Chem. Soc.* 119, 12069–12088.
- Berti, P. J. (1999) *Methods Enzymol.* 308, 355–397.
- Fasman, G. D. (1975) in *Handbook of Biochemistry and Molecular Biology: Nucleic Acids Vol. 1*, CRC Press, Boca Raton, FL.
- Stivers, J. T. (1998) *Nucleic Acids Res.* 26, 3837–3844.
- Gilles, A.-M., Cristea, I., Palibroda, N., Hilden, I., Jensen, K. F., Sarfati, R. S., Namane, A., Ughetto-Monfrin, J., and Barzu, O. (1995) *Anal. Biochem.* 232, 197–203.
- Serina, L., Blondin, C., Krin, E., Sismeiro, O., Danchin, A., Sakamoto, H., Gilles, A.-M., and Barzu, O. (1995) *Biochemistry* 34, 5066–5074.
- Jensen, K. F., and Mygind, B. (1996) *Eur. J. Biochem.* 240, 637–645.
- Switzer, R. L., and Gibson, K. J. (1978) *Methods Enzymol.* 51, 3–17.
- Bradford, B. B. (1976) *Anal. Biochem.* 72, 248.
- Stubbe, J., Smith, G., and Blakley, R. (1983) *J. Biol. Chem.* 258, 1619–1624.
- Brinkley, S. A., Lewis, A., Critz, W. J., Witt, L. L., Townsend, L. B., and Blakley, R. L. (1978) *Biochemistry* 17, 2350–2356.
- Joyce, C. M., and Grindley, N. D. F. (1983) *Proc. Natl. Acad. Sci. U.S.A.* 80, 1830–1834.
- Stivers, J. T., Jagadeesh, G. J., Nawrot, B., Stec, W. J., and Shuman, S. (2000) *Biochemistry* 39, 5561–5572.
- Sekiguchi, J., and Shuman, S. (1997) *Mol. Cell* 1, 89–97.
- Parkin, D. W. (1991) in *Enzyme Mechanism from Isotope Effects*, CRC Press, Boca Raton, FL.
- Bigeleisen, J., and Wolfsburg, M. (1958) *Adv. Chem. Phys.* 1, 15.
- Leatherbarrow, R. J. (1998) *GraFit 4.0*, Erithacus Software Ltd., Staines, U.K.
- Rose, I. A. (1995) *Methods Enzymol.* 249, 315–340.
- Zimmer, D. P., and Crothers, D. M. (1995) *Proc. Natl. Acad. Sci. U.S.A.* 92, 3091–3094.
- Moran, S., Ren, R. X.-F., Sheils, C. J., Rumney, S. I., and Kool, E. T. (1996) *Nucleic Acids Res.* 24, 2044–2052.
- Cleland, W. W. (1982) *CRC Crit. Rev. Biochem.* 13, 385–428.
- Duggleby, R. G., and Northrop, D. B. (1989) *Bioorg. Chem.* 17, 177–193.
- Schramm, V. L. (1991) in *Enzyme Mechanism from Isotope Effects* (Cook, P. F., Ed.) CRC Press, Boca Raton, FL.
- Goitein, R. K., Chelsky, D., and Parsons, S. M. (1978) *J. Biol. Chem.* 253, 2963–2971.
- Guthrie, R. D., and Jencks, W. P. (1989) *Acc. Chem. Res.* 22, 343–349.
- Hehre, W. J. (1975) *Acc. Chem. Res.* 8, 369–376.
- Sunko, D. E., Szele, I., and Hehre, W. J. (1977) *J. Am. Chem. Soc.* 99, 5000–5005.
- Ashwell, M., Guo, X., and Sinnott, M. L. (1992) *J. Am. Chem. Soc.* 114, 10158–10166.
- Huang, X. C., Surry, C., Hiebert, T., and Bennet, A. J. (1995) *J. Am. Chem. Soc.* 117, 10614–10621.
- Huang, X., Tanaka, K., and Bennet, A. J. (1997) *J. Am. Chem. Soc.* 119, 11147–11154.
- Zhu, J., and Bennet, A. J. (1998) *J. Am. Chem. Soc.* 120, 3887–3893.
- Schramm, V. L. (1998) *Annu. Rev. Biochem.* 67, 693–720.
- Melander, L., and Saunders, W. H. (1980) in *Reaction Rates of Isotopic Molecules*, Wiley, New York.
- Berti, P. J., Blanke, S. R., and Schramm, V. L. (1997) *J. Am. Chem. Soc.* 119, 12079–12088.
- Scheuring, J., Berti, P. J., and Schramm, V. L. (1998) *Biochemistry* 37, 2748–2758.
- Tao, W., Grubmeyer, C., and Blanchard, J. S. (1996) *Biochemistry* 35, 14–21.
- Scheuring, J., and Schramm, V. L. (1997) *Biochemistry* 36, 8215–8223.
- Rising, K. A., and Schramm, V. L. (1997) *J. Am. Chem. Soc.* 119, 27–37.
- Kline, P. C., and Schramm, V. L. (1993) *Biochemistry* 32, 13212–13219.
- Horenstein, B. A., Parkin, D. W., Estupinan, B., and Schramm, V. L. (1991) *Biochemistry* 30, 10788–10795.
- Parkin, D. W., and Schramm, V. L. (1987) *Biochemistry* 26, 913–920.
- Markham, G. D., Parkin, D. W., Mentch, F., and Schramm, V. L. (1987) *J. Biol. Chem.* 262, 5609–5615.
- Zhang, Y., Bommuswamy, J., and Sinnott, M. L. (1994) *J. Am. Chem. Soc.* 116, 7557–7563.
- Tanaka, Y., Tao, W., Blanchard, J. S., and Hehre, E. J. (1994) *J. Biol. Chem.* 269, 32306–32312.
- Basti, M. M., Stuart, J. W., Lam, A. T., Guenther, P., and Agris, F. (1996) *Nat. Struct. Biol.* 3, 38.

BI0018178